Open Chem., 2015; 13: 161–171

Research Article **Open Access**

Agnieszka Pilarska, Karol Bula, Kamila Myszka, Tomasz Rozmanowski, Karolina Szwarc-Rzepka, Krzysztof Pilarski, Łukasz Chrzanowski, Katarzyna Czaczyk, Teofil Jesionowski*

Functional polypropylene composites filled with ultra-fine magnesium hydroxide

Abstract: Magnesium hydroxide was prepared under controlled conditions from aqueous $Mg(NO_3)_2$ and NaOH solutions. The small, nanoplate-shaped particle size distribution was monomodal from 164 to 459 nm. Functional polypropylene/$Mg(OH)_2$ and polypropylene/polypropylene 1% maleic anhydride/$Mg(OH)_2$ composites were prepared containing 10% or 30% $Mg(OH)_2$. The composites have a high Young's modulus (twice that of polypropylene) and comparable tensile strength but less ductility. EDX examination of the fractured composite surfaces suggested a homogeneous $Mg(OH)_2$ distribution for composites produced with the addition of polypropylene grafted with maleic anhydride. The polypropylene/$Mg(OH)_2$ composites showed good antibacterial activity. The polypropylene/polypropylene 1% maleic anhydride/$Mg(OH)_2$ composites were less effective.

Keywords: magnesium hydroxide, polypropylene composites, flame retardant, mechanical and antibacterial properties

DOI: 10.1515/chem-2015-0024
received February 17, 2014; accepted July 07, 2014.

***Corresponding author: Teofil Jesionowski:** Institute of Chemical Technology and Engineering, Faculty of Chemical Technology, Poznan University of Technology, PL-60965 Poznan, Poland, E-mail: Teofil.Jesionowski@put.poznan.pl
Agnieszka Pilarska, Karolina Szwarc-Rzepka, Łukasz Chrzanowski: Institute of Chemical Technology and Engineering, Faculty of Chemical Technology, Poznan University of Technology, PL-60965 Poznan, Poland
Karol Bula: Institute of Materials Technology, Faculty of Mechanical Engineering and Management, Poznan University of Technology, PL-61138 Poznan, Poland
Kamila Myszka, Katarzyna Czaczyk: Department of Biotechnology and Food Microbiology, Faculty of Food Science and Nutrition, Poznan University of Life Sciences, PL-60627 Poznan, Poland
Tomasz Rozmanowski: Institute of Chemistry and Technical Electrochemistry, Faculty of Chemical Technology, Poznan University of Technology, PL-61138 Poznan, Poland
Krzysztof Pilarski: Institute of Biosystems Engineering, Faculty of Agriculture and Bioengineering Poznan University of Life Science, PL-60637 Poznan, Poland

1 Introduction

Magnesium hydroxide has been used to neutralize pollutants [1], in pharmaceutical production [2,3], in fertilizers [4], as a paper preservative [5], and as a magnesium oxide precursor [6–8]. Its varied morphology, hydrophilicity, basicity, non-toxicity and antibacterial activity have recently stimulated new applications, ranging from membrane production, [9] biomaterials [2], compound detection [10] to modern polymer composites [11–16]. Its uses as a flame retardant [15–22] and as an antibacterial agent [23–27] are areas of active research.

Non-toxicity and high thermal stability make magnesium hydroxide particularly attractive in reducing polymer flammability. The thermal stability allows it to be combined with epoxy resins [14] in addition to its classical composites with ethylene vinyl acetate (EVA), polypropylene (PP) and polyethylene (PE). However, $Mg(OH)_2$ has a low efficiency as a flame retardant and the high concentration necessary may impair the mechanical properties of the resulting composite.

Surface modification of $Mg(OH)_2$ may improve its compatibility. For example, a nano-$Mg(OH)_2$/EVA composite with synergistic microcapsulated red phosphorus has been proposed. Thermogravimetric and spectroscopic analysis have examined its flame retardant mechanism [21]. $Mg(OH)_2$ modified with zinc titanate and stearate has been evaluated as a potential halogen-free flame retardant filler for polypropylene [12]. The flame retardant effect of magnesium hydroxide in epoxy resins has also been assessed. The work examined how the $Mg(OH)_2$ particle size and surface modifications with silanes affected the flame retardant, thermal and mechanical properties. Even in small quantities $Mg(OH)_2$ with small particle sizes can achieve similar or superior flame retardant performance compared with mico-sized particles [14].

The primary reason for microorganisms surface adhesion is to gain the stability required for colonization of new sites. This is especially true of opportunistic pathogens such as *Pseudomonas aeruginosa*, which

adhere to implants and live tissue [28]. The virulence displayed by this taxon is mostly associated with the secretion of polymeric substances such as rhamnolipids, which promote bacterial motility as well as cellular adherence and subsequent biofilm formation [29]. This bacterium is often used to test antimicrobial activity.

Antibiotic resistance has promoted increasing interest in alternatives [30]. Functionalized nanoparticles are among the most popular and novel solutions to this problem [31,32]. Traditionally, silver or copper has been used to disrupt microbial metabolism and limit infection. Nanoparticle-based materials continually provide metal ions, which decrease the microbe activity. Magnesium hydroxide acts in this way; it is also cheap and non-toxic. Active nano-$Mg(OH)_2$ can be an especially effective antibacterial.

The main aim of this work was to test the flame retardant effectiveness of $Mg(OH)_2$ of excellent dispersive properties in $PP/Mg(OH)_2$ composites, and to evaluate their mechanical and antibacterial properties. The expected high fire retardancy and high antibacterial activity is not due to expensive substrates or time and labor consuming synthesis but to the use of high quality inorganic filler. The completely non-toxic properties of $Mg(OH)_2$ contrast with the popular organic flame retardants based on halogens, halogen and phosphorus, or phosphonates. Such composites can be used for objects of everyday use as well as food and pharmaceutical packaging.

2 Experimental procedure

2.1 Large-scale laboratory $Mg(OH)_2$ synthesis

Magnesium hydroxide was precipitated under several dozen conditions of temperature, concentration and reagent ratio, speed and method of addition, and drying. Each set of conditions was repeated three times. In the optimized procedure, precipitation was carried out in a 10-liter reactor (NORMAG Labor- und Prozesstechnik GmbH) fitted with a fast rotating paddle mixer (Chiaravalli Transmissioni SPA) at 40°C, maintained by water circulation between the reactor outer jacket and a water bath. Using a peristaltic pump, 10% magnesium nitrate and stoichiometric amounts of sodium hydroxide were added simultaneously at a constant rate to water in the reactor. The resulting precipitate was washed, filtered, and dried at 105°C for approximately 8 h (Fig. 1). Figure 1 shows the $Mg(OH)_2$ preparation.

2.2 $PP/Mg(OH)_2$ composites production

The $PP/Mg(OH)_2$ composites were made using isotactic polypropylene homopolymer (Moplen HP 500J) with a melt flow index of 3.2 g per 10 min at 230°C (no antiblocking or clarifying agents) and polypropylene grafted with 1% maleic anhydride (PP-*g*-MAH) with a melt flow index of 111.5 g per 10 min at 190°C (Polybond 3200). Composites with 10 wt% or 30 wt% $Mg(OH)_2$ and 10% PP-g-MAH were prepared by extrusion with polypropylene in a twin-screw extruder with 16 mm screw diameter and L/D ratio 40. The plasticizing temperature was 170–210°C, with a screw speed of 150 rpm. The extruder gave very good sample homogeneity. An ENGEL ES-80/20 injection molder was used (injection speed 110 mm/s, mold temperature 25°C, plasticizing temperature 180–215°C). Dumbbell-shaped specimens (150×10×4 mm) were used to analyse the tensile properties and 125×10×4 mm rectangular specimens were used to test flammability.

2.3 Analysis of $Mg(OH)_2$ and $PP/Mg(OH)_2$

Magnesium hydroxide particle size distributions were determined using a Nano ZS Zetasizer (Malvern Instruments), permitting measurements of 0.6–6000 nm particle diameters by laser backscattering. The sample was prepared by dispersing 0.01 g of the product in 25 mL of isopropanol, stabilizing in an ultrasonic bath for 15 minutes, and placing in a cuvette. The instrument passes a 663 nm red laser beam through the sample and measures the fluctuations in scattered light intensity due to the particles' Brownian motion. The surface morphology and microstructure of $Mg(OH)_2$ and $PP/Mg(OH)_2$ were examined by an EVO40 scanning electron microscope (Zeiss). Before testing the samples were Au coated for 5 s using a Balzers PV205P coater. The presence of magnesium hydroxide functional groups was shown by a Vertex 70 FT-IR (Bruker, Germany) from 4000–400 cm^{-1} (resolution of 0.5 cm^{-1}) using KBr pastil. Thermal analysis of the magnesium hydroxide and composites was performed using a Jupiter 449 F3 (Netzsch GmbH, Germany). Approximately 10.0 mg samples were heated in alumina pans from 30 to 1000°C at 10°C min^{-1} under flowing nitrogen at 40 mL min^{-1}. The surface composition was determined by energy dispersion spectroscopy (EDS) using a PGT Avalon X-ray microanalyser with a Si (Li) detector with ultra-thin window and a 20 kV accelerating voltage. The samples were coated with a thin layer of carbon. Standardless quantitative analysis and ZAF matrix correction algorithms for SEM bulk analysis were applied.

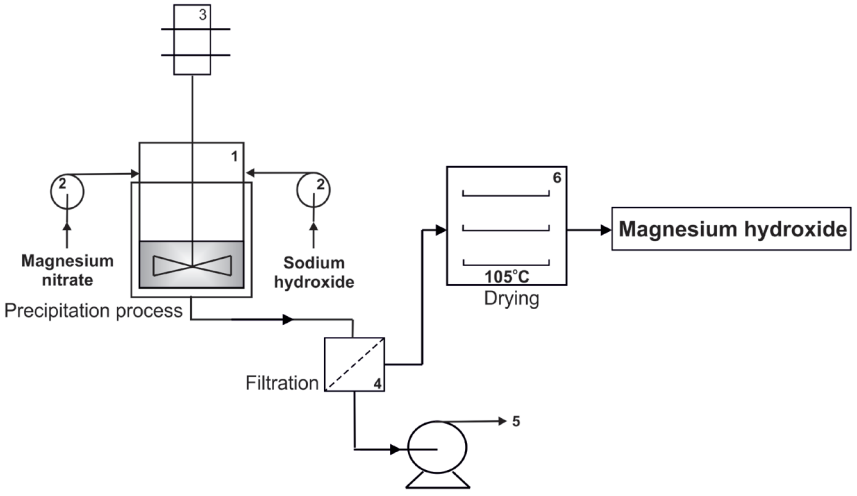

Figure 1: Magnesium hydroxide preparation. 1 – reactor; 2 – peristaltic pump; 3 – stirrer; 4 – pressure filter; 5 – vacuum pump; 6 – drier.

2.4 Testing of flame retardant and mechanical properties of PP/$Mg(OH)_2$ composites

The composites' flammability was tested using the UL94 H-B horizontal combustion method, where a linear rate of combustion is determined for a horizontally placed sample. The samples were heated using a 50 W burner at an angle of 45°. After the elapse of 30 s the time taken for the flame to reach a boundary of 75 mm, starting from a boundary of 25 mm was measured. The reference material was pure polymer tested under identical conditions.

Composite tensile analysis was carried out by single-axis extension (crosshead speed 50 mm min^{-1}) using an Instron model 4481 with self-clamping action grip and 50 kN head capacity. Following ISO 527-2 the yield strength, tensile strength, Young's modulus and elongation at break were determined .

2.5 PP/$Mg(OH)_2$ composites' antibacterial properties

Pseudomonas aeruginosa strain ATCC 10145 obtained from the American Type Culture Collection (Rockville, MD, USA) was used for testing. The microorganisms were grown for 48 h at 37°C under shaking (100 rpm) in an LB medium (peptone 10 g L^{-1}; yeast extract 5 g L^{-1}; NaCl 5 g L^{-1}; pH 7.0; Bretani [33]). Shaped specimens (pure $Mg(OH)_2$ and PP/$Mg(OH)_2$ composites) were placed in liquid cultures. After 4, 8, 24 and 48 h the samples were removed and washed with pH 7.2 phosphate buffered saline to remove any cells temporarily attached. The shaped specimens and foils were stained with 0.01% acridine orange and examined by fluorescent microscopy (CARL-ZEISS, Axiovert 200, Germany). The degree of bacterial surface adhesion was determined by the method of Le Thi and Prigent-Combaret [34]. In this technique, 50 visual fields are assessed on a 9-point scale based on the following definitions: (i) 1st degree: from 0 to 5 bacterial cells in the visual field; (ii) 2nd degree: from 5 to 50 bacterial cells in the visual field; (iii) 3rd degree: only single bacterial cells (above 50 bacterial cells in the visual field), no microcolonies; (iv) 4th degree: single bacterial cells + macrocolonies; (v) 5th degree: large but not confluent microcolonies + single bacterial cells; (vi) 6th degree: confluent microcolonies + single bacterial cells; (vii) 7th degree: 1/4 of the visual field covered by the biofilm; (viii) 8th degree: 1/2 of the visual field covered by the biofilm; (ix) 9th degree: visual field totally covered by the biofilm.

3 Results and discussion

3.1 Dispersive and morphological properties of $Mg(OH)_2$ filler

The product exhibited the small particle size and high homogeneity favorable to composite formation. These properties, in particular the high homogeneity, are achieved by process parameter selection. The properties of the $Mg(OH)_2$ used remained unchanged following scale up from ordinary laboratory scale to large laboratory scale, which is significant for applications.

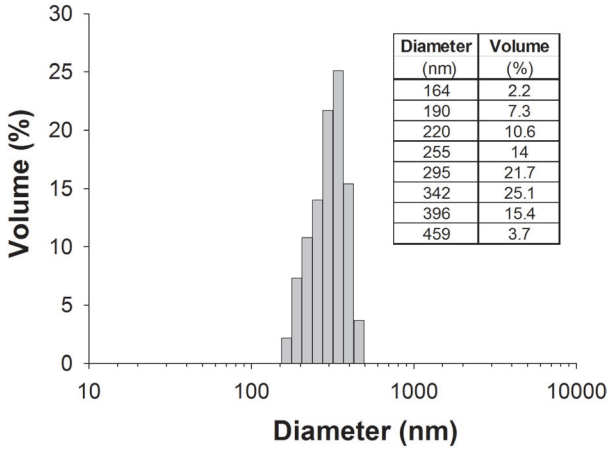

Diameter (nm)	Volume (%)
164	2.2
190	7.3
220	10.6
255	14
295	21.7
342	25.1
396	15.4
459	3.7

Figure 2: Particle size of magnesium hydroxide precipitated by 10% magnesium nitrate at 40°C.

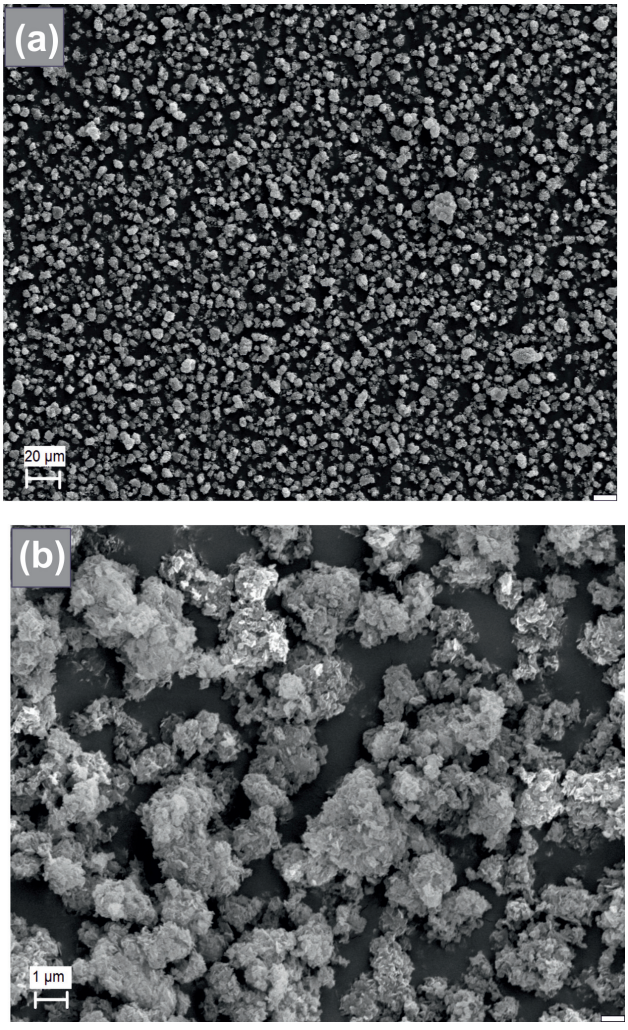

Figure 3: SEM of magnesium hydroxide.

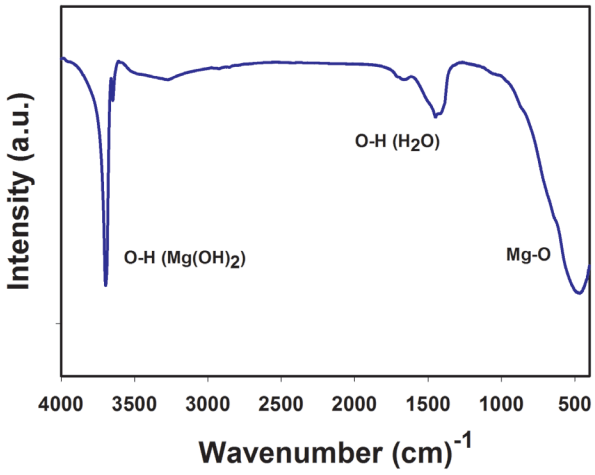

Figure 4: FT-IR of magnesium hydroxide.

The particle size distribution (Fig. 2) was monomodal from 164 to 459 nm. The SEM (Figs. 3a, 3b) shows small, nanoplate-shaped particles.

The relatively small plate-like particles (Figs. 2 and 3) suggest success when used as both flame retardant and as antibacterial agent

3.2 Chemical and thermal analysis of $Mg(OH)_2$ filler

The sharp and intense 3700 cm^{-1} FT-IR peak (Fig. 4) corresponds to $Mg(OH)_2$ asymmetric O–H stretching. The band at 1650 cm^{-1} is due to the water O–H stretch. The strong and wide 440 cm^{-1} peak is due to Mg–O stretching. These agree with the literature [35].

Based on TGA, the composition of the sample was assessed and the temperatures of $Mg(OH)_2$ decomposition were determined. At the first stage (Fig. 5) there is a small mass loss (*ca.* 2%) due to the endothermic loss of physically bound water [36]. Further rapid mass loss (25% up to 390°C and 28% up to 550°C) is due to $Mg(OH)_2$ decomposition, loss of water of crystallization, and formation of the MgO structure. The mass stabilizes at 800°C. According to the DTG curve, the greatest mass loss occurs from 250°C to 410°C. These results agree with previous work [18,37,38].

3.3 Chemical and morphological properties of PP/$Mg(OH)_2$ composites

The PP/$Mg(OH)_2$ composites were prepared using 10 wt% or 30 wt% of precipitated magnesium hydroxide and a polypropylene grafted with maleic anhydride

modifier. EDS was used to determine the composition of unmodified and modified composites (Table 1, Fig. 6). Fig. 6a corresponds to pure PP, while Figs. 6b, c show the composition of composites with PP-g-MAH addition.

Samples with greater $Mg(OH)_2$ content contain more oxygen and magnesium while in modified composites there is a slightly higher carbon content (Table 1). The elemental distribution for PP/10% $Mg(OH)_2$ is shown by EDS maps. Carbon has the highest density (Table 1, Fig. 7a), while oxygen and magnesium densities are much less (Figs. 7b-7d). Figs. 7c, 7d show a relatively homogeneous system, with visible agglomerates of higher magnesium concentration. Filler agglomerates are undesirable; often impairing composite mechanical properties.

Figs. 8 and 9 are SEM images of PP/10% $Mg(OH)_2$ (Fig. 8) and PP/30% $Mg(OH)_2$ (Fig. 9) composites compatibilized with or without PP-g-MAH. Figures a and b are of the same sample; c and d are a different one. Images b and c were acquired using back-scattered electrons. Examination of the images suggests that 10% filler in the matrix ensures uniform dispersion. The cryo-fractured composite morphology indicates a similar degree of microfiller dispersion in the presence and in the absence of the compatibilizer. Figs. 8a, 8b and Figs. 8c, 8d reveal the presence of similarly sized small agglomerates. The presence of 30% $Mg(OH)_2$ (Fig. 9) has a different effect. The SEM images of unmodified composites (Figs. 9c, 9d) show

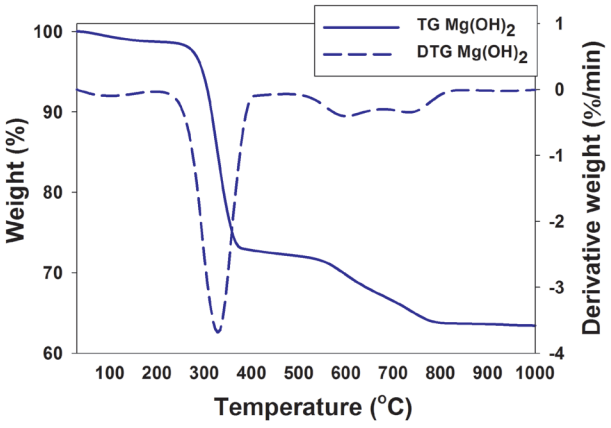

Figure 5: TG and DTG of magnesium hydroxide.

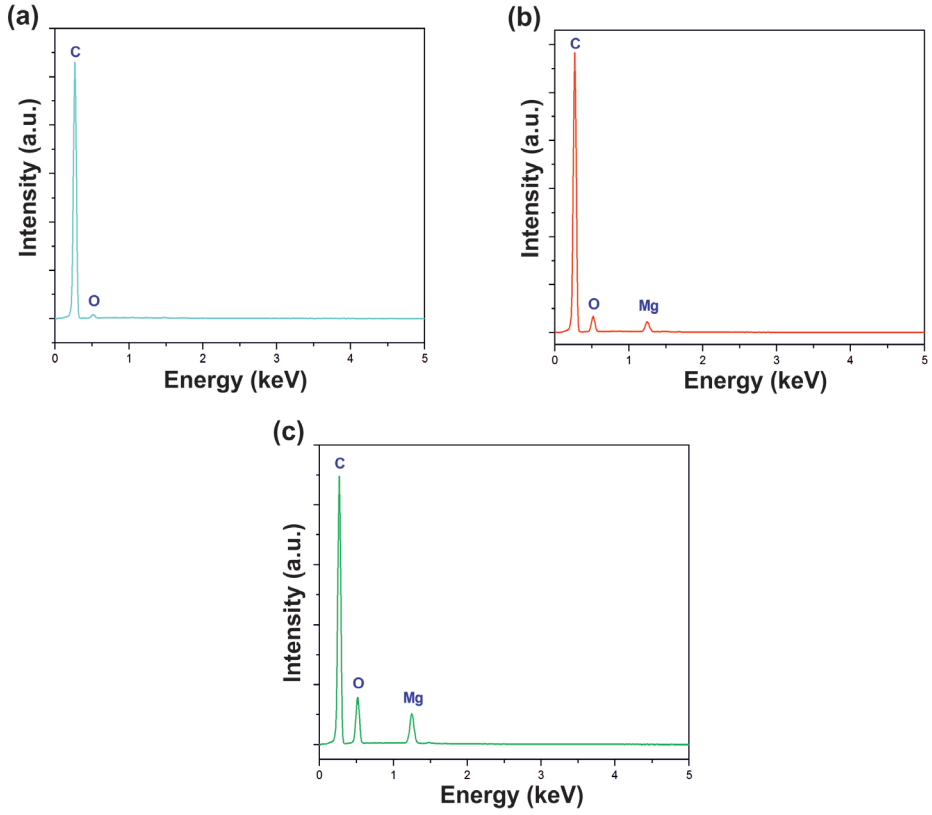

Figure 6: Surface composition of (a) pure PP, (b) PP/PP-g-MAH/10%$Mg(OH)_2$, (c) PP/PP-g-MAH/30%$Mg(OH)_2$.

Table 1: Chemical composition of pure PP and tested composites.

Material	Elements content* (%)					
	wt. (%)			at. (%)		
	C	O	Mg	C	O	Mg
PP	95.24	4.72	–	96.61	3.09	–
PP/10%$Mg(OH)_2$	78.05	18.08	2.80	85.07	12.53	0.97
PP/30%$Mg(OH)_2$	69.22	24.91	4.00	76.26	21.10	2.21
PP/10%*PP-g-MAH/10%$Mg(OH)_2$	84.51	13.34	1.70	88.43	10.48	0.16
PP/10%*PP-g-MAH/30%$Mg(OH)_2$	69.78	25.40	4.63	76.51	20.91	2.51

*samples may also contain small quantities of impurities in the form of aluminium or silicon
* concentration of PP-g-MAH (polypropylene grafted with maleic anhydrite)

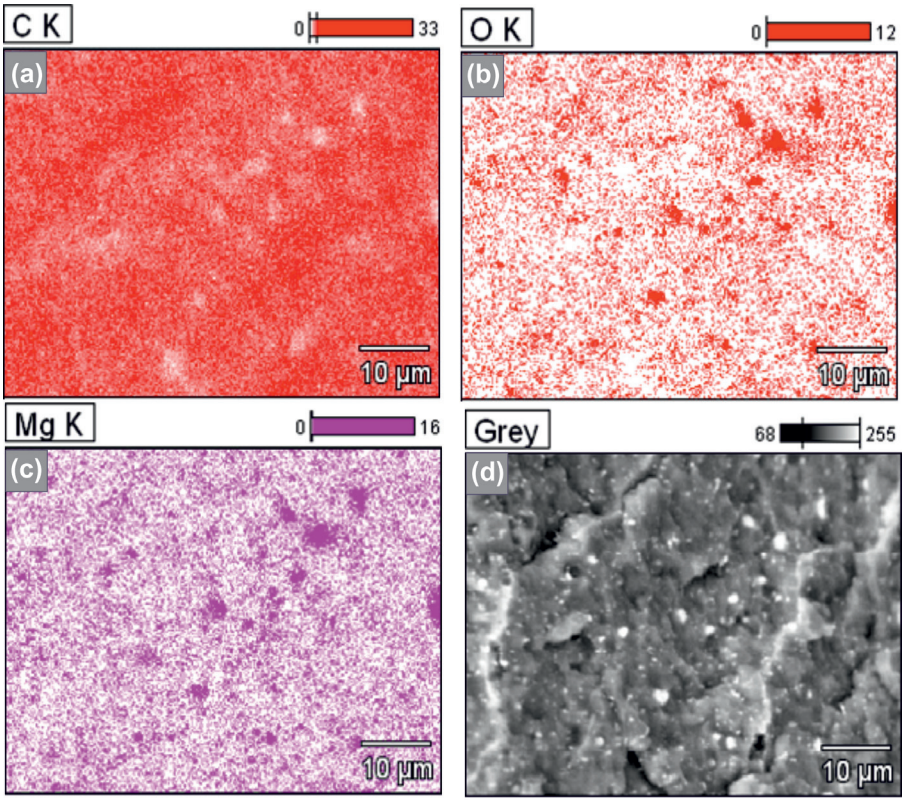

Figure 7: X-ray maps of (a) carbon; (b) oxygen; (c, d) magnesium.

large agglomerates of non-uniform shapes and sizes. This indicates that higher compatibilizer contributions should be used to decrease the interfacial stress, increase wetting by the polymer, and improve filler dispersion. SEM images of the fractured surfaces of composites containing maleic anhydride (Fig. 9a, 9b) confirmed the improved mixing and reduced agglomeration. Figs. 9a, 9b (PP/10% PP-g-MAH/30% $Mg(OH)_2$) show an even filler distribution with a slight tendency to form small agglomerates. The simultaneous use of a twin-screw extruder and a polymer grafted with maleic anhydride compatibiliser reduced the agglomerate quantity and size [39,40].

Long mixing or the use of a modifier will not guarantee homogeneous inorganic filler dispersion in the polymer matrix. Carrot *et al.* [16] determined that tension at the phase boundary leads to deformation of the interphase surface causing magnesium hydroxide agglomeration in a molten olefin polymer. The resulting agglomerates are moistened by the polymer, form a kind of separate phase, and can be easily deformed. The rheology of a polymer filled with $Mg(OH)_2$ is also affected by the polymer viscosity and filler quantity.

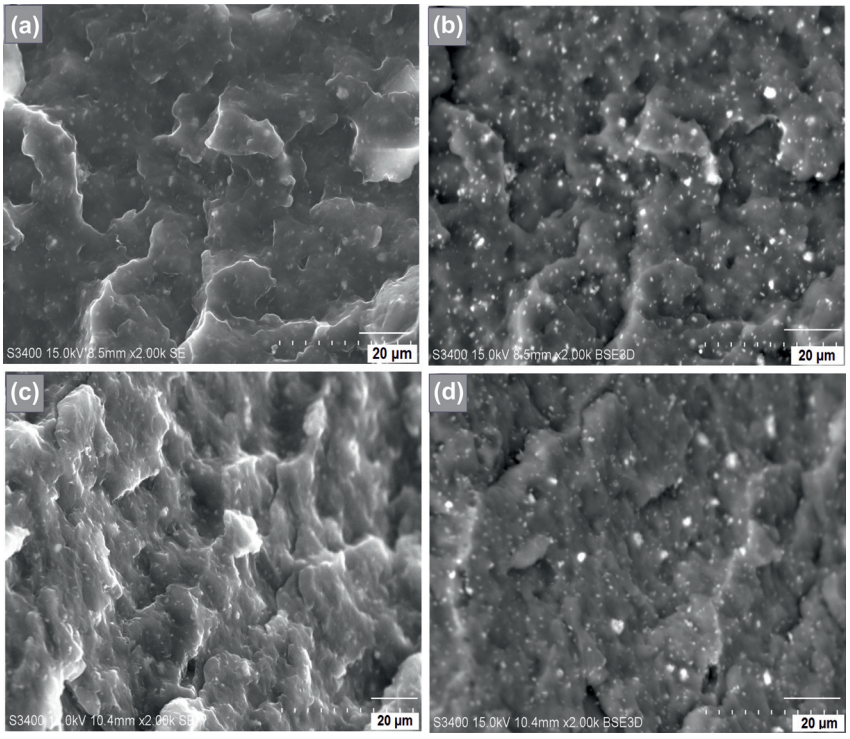

Figure 8: SEM of (a, b) (SE) modified PP/10% $Mg(OH)_2$ and (c, d) (BSE) unmodified PP/PP-g-MAH/10%$Mg(OH)_2$.

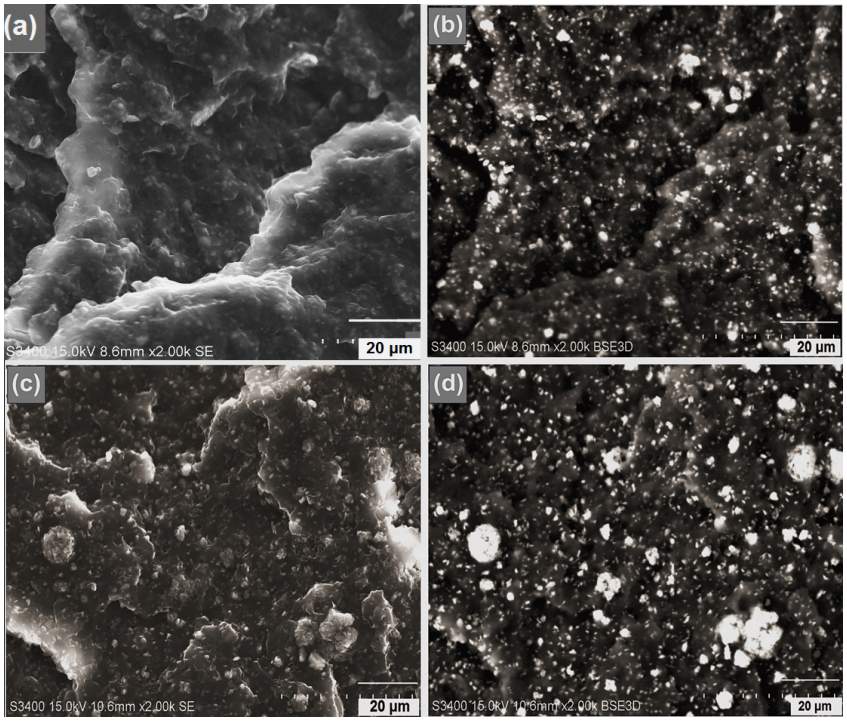

Figure 9: SEM of (a, b) (SE) modified PP/30% $Mg(OH)_2$ and (c, d) (BSE) unmodified PP/PP-g-MAH/30%$Mg(OH)_2$.

Table 2: Mechanical properties of the unmodified composites PP/$Mg(OH)_2$ and contained PP-g-MAH.

Material	Yield strength (MPa)	Tensile strength (MPa)	Young modulus (MPa)	Elongation at break (%)
PP	17.5 ± 0.4	33 ± 0.3	697 ± 28	120 ± 16
PP/10%$Mg(OH)_2$	20 ± 0.5	34 ± 0.6	898 ± 17	65 ± 22
PP/30%$Mg(OH)_2$	15 ± 0.3	33 ± 0.2	1152 ± 22	13.8 ± 11
PP/10%PP-g-MAH/10%$Mg(OH)_2$	19 ± 0.7	35 ± 0.2	887 ± 18	60 ± 4
PP/10%PP-g-MAH/30%$Mg(OH)_2$	16 ± 0.6	37 ± 0.4	1304 ± 18	16.5 ± 0.9

3.4 Mechanical properties of PP/$Mg(OH)_2$ composites

Adding $Mg(OH)_2$ to a polymer matrix changes the material's tensile parameters. Introduction of a large proportion of magnesium hydroxide (PP/30% $Mg(OH)_2$ and PP/10% PP-g-MAH/30% $Mg(OH)_2$) causes a marked fall in elongation at break, from 120±16% to 13.8±11% and 16.5±0.9% (Table 2). This increased brittleness is consistent with microscopic observation of large filler agglomerates. On the other hand, samples with a 30% $Mg(OH)_2$ content display high values of Young's modulus, almost twice as great as for unfilled PP (calculated by the Bluehill 2.0 software). This high value is because binding magnesium hydroxide to PP increases the rigidity due to reduction in the mobility of the attached macromolecules in the presence of maleic anhydride [38]. The composites tensile strengths are comparable to or slightly higher than polypropylene (36±0.4 MPa for PP/10% PP-g-MAH/30% $Mg(OH)_2$). Addition of PP-g-MAH gives slightly better mechanical properties.

Suihkonen *et al.* [14] examined a similar problem. $Mg(OH)_2$ silanization using 3-aminopropyltriethoxysilane produced unfavorable results: there was an increase in the Young's modulus but a fall in the values of the other mechanical parameters, including by 40% for elongation at break. Gul *et al.* [13] also observed a dramatic fall in this parameter (from 111.6% to 1.3%). Such unfavourable results are comparable to those obtained here (Table 2) and indicate brittleness. This is obviously a key problem in modifying agent selection [11–14,18,21].

3.5 Flame retardant and thermal properties of PP/$Mg(OH)_2$ composites

The results in Table 3 confirm a significant reduction in combustion rate with increasing inorganic filler content. The addition of 30% magnesium hydroxide produced the largest fall in combustion rate. The slowest-burning material was produced from a pre-mixture with maleic anhydride (PP/10% PP-g-MAH/30% $Mg(OH)_2$), which gave the largest change (42%) relative to pure polypropylene. This is a result of the substantial flame retardant content as well as the more homogeneous mixture containing PP-g-MAH, which improved the polymer - magnesium hydroxide affinity (Figs. 9c, 9d). This retarded the polymer softening and macromolecule migration to the combustion zone. In transverse combustion tests systems with added $Mg(OH)_2$ produce less smoke than pure polypropylene. Unfilled polypropylene drips because the viscosity drops when heated. The filler significantly reduces this, probably because polymer chains are immobilized and thermal decomposition is delayed.

Table 3: Composite linear combustion rates (UL 94 method).

Material	Linear rate of combustion V=60 L/t (mm min^{-1})	Changes relative to PP (%)
PP	24.3	–
PP/10%$Mg(OH)_2$	22.2	8.6
PP/30%$Mg(OH)_2$	17.5	28
PP/10%PP-g-MAH/10%$Mg(OH)_2$	22.9	5.8
PP/10%PP-g-MAH/30%$Mg(OH)_2$	14.1	42

The expected reduction in the polypropylene combustion rate is due to formation of a dense carbonized layer which inhibits diffusion of the flammable gaseous pyrolysis products. The reductions in diffusion and in heat conduction across the carbonized layer reduce the combustion rate. These phenomena depend primarily on homogeneous filler dispersion. For the material modified with maleic anhydride, PP/10% PP-g-MAH/30% $Mg(OH)_2$, the rate reduction from 24.3 mm min^{-1} to 14.1 mm min^{-1} and the 42% decrease compared to pure polypropylene are significant compared with literature data [11–13,37].

TG and DTG analysis determined the mass loss caused

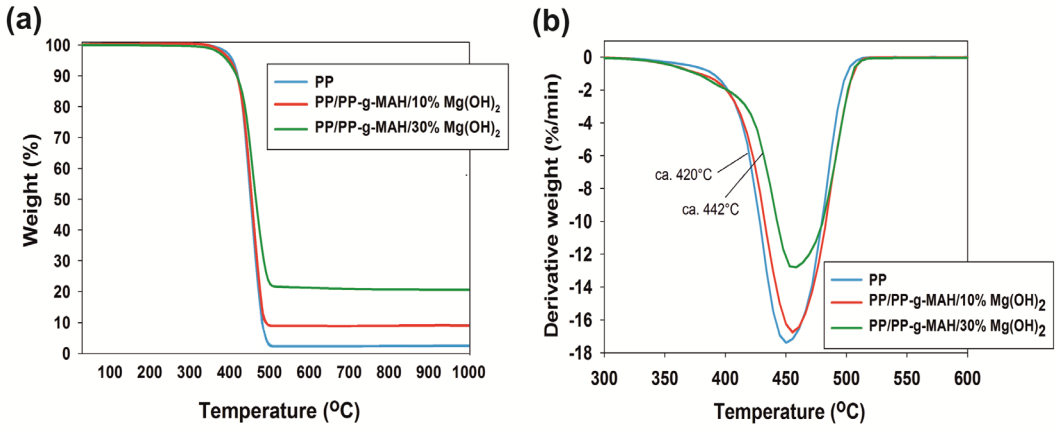

Figure 10: (a) TG, (b) DTG of PP and PP/PP-g-MAH/10%$Mg(OH)_2$, PP/PP-g-MAH/30%$Mg(OH)_2$ composites.

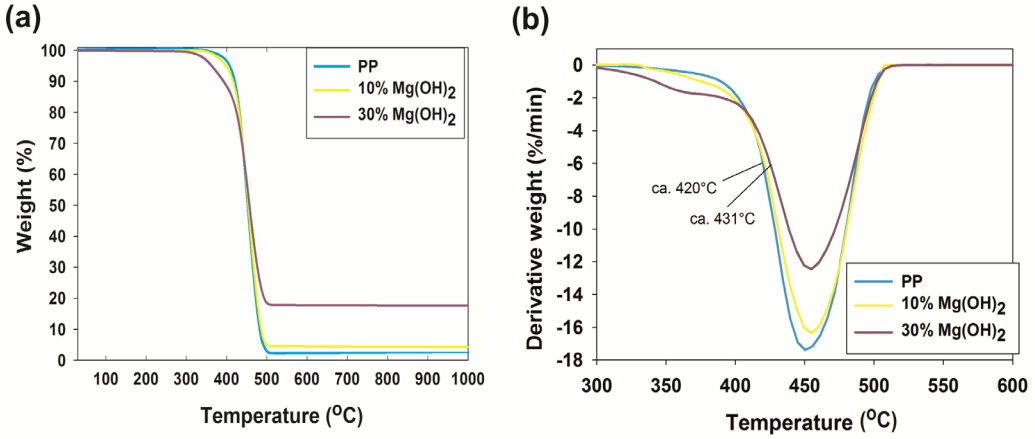

Figure 11: (a) TG, (b) DTG of PP and PP/10% $Mg(OH)_2$, and PP/30% $Mg(OH)_2$ composites.

by heat (a basis for evaluation of resistance to thermal decomposition), and to compare temperatures at which decomposition began [13,14,18,37]. The TG and DTG curves shown in Figs. 10 and 11 allow $Mg(OH)_2$ and MAH modifier effectiveness evaluation.

The thermogravimetric curve shapes (Figs. 10a, 11a) indicate that neat PP and PP/PP-g-MAH/$Mg(OH)_2$ composites show one-step weight loss. The curves in Fig. 10a are very similar in shape, but the PP/PP-g-MAH/30% $Mg(OH)_2$ decomposition temperatures are slightly higher than for PP. The thermal stability of PP highly loaded with $Mg(OH)_2$ in the presence of maleated polypropylene is superior to that of the neat PP. Figs. 11a and 11b imply that PP/30% $Mg(OH)_2$ without compatibiliser shows an unlikely two-step weight loss under flowing nitrogen. Aggregated and poorly-dispersed $Mg(OH)_2$ particles would decompose by water release more readily, leading to a slight increase in weight loss at around 365°C. For further investigation TGA should be done under air flow [41,42].

The large surface area of homogeneous fine magnesium hydroxide (Figs. 2, 3) strongly blocks the movement of macromolecules and delays the decomposition, shifting it to higher temperatures. The DTG (Figs. 10b, 11b) shows a marked curve shift for systems containing 30% $Mg(OH)_2$.

The DTG graphs (Figs. 10b, 11b) which show very similar maximum mass loss rate peak locations for all systems. However, a slight peak shift was observed in PP/PP-g-MAH/30% $Mg(OH)_2$ compared to the PP resin.

Gul *et al.* [13] confirmed synergism among magnesium hydroxide, sepiolite, and polyethylene. Composite thermal stability increased with increasing sepiolite concentration; fire resistance improved by 21.2°C. Balakrishnan *et al.* [37] found that addition of 50% $Mg(OH)_2$ to polyamide 6/polypropylene shifted the curves to higher temperatures by as much as 40.02°C.

Table 4: Dominating and higher adhesion degrees of *Pseudomonas aeruginosa* to the composites surface.

Material	Incubation time (h)	Dominating adhesion degree	The presence of higher adhesion degree (6,7,8,9)
$Mg(OH)_2$	4	1	–
	24	1	–
PP/10%$Mg(OH)_2$	4	1	–
	24	1	–
PP/30%$Mg(OH)_2$	4	1	–
	24	1	–
PP/10%PP-g-MAH/10%$Mg(OH)_2$	4	2,4	6
	24	4	7
PP/10%PP-g-MAH/30%$Mg(OH)_2$	4	2	6
	24	4	6

3.6 Antibacterial properties of $Mg(OH)_2$ composites

The antibacterial activity of precipitated $Mg(OH)_2$ was evaluated by determining the degree of bacterial adhesion [34]. Adhesion was assumed dominant when it was at least 20%.

Table 4 shows that degree 1 adhesion dominates for unmodified PP/$Mg(OH)_2$ composites after 4 and 24 hours. This demonstrates the high activity of the synthesized magnesium hydroxide, both in pure form and in combination with polymer; this may prove key to applications of this filler. Maleic anhydride modifier has unfavourable effects on composite antibacterial activity. Its addition (with either 10 and 30 wt% $Mg(OH)_2$) caused increased adhesion (degrees 2, 4 after 4 hours and 6, 7 after 24 hours), leading to micro- and macrocolonies and, at a further stage, of biofilm.

Effective antibacterial activity of nano-$Mg(OH)_2$ against *Escherichia coli* has recently been reported by Dong *et al.* [24]. They also attribute the high antibacterial activity not just to dissolved Mg^{2+} or OH^- ions but to the nanoplate structure. Direct bacterial contact with the nanoplates is assumed responsible for their death. The antibacterial effectiveness of $Mg(OH)_2$ also depends on its particle size [43], confirmed by this work (Figs. 2 and 3). Dong *et al.* also showed that the hydroxide markedly reduced the growth and activity of *Escherichia coli* and *Burkholderia phytofirmans* [25]. They proposed two mechanisms for this effect. The first assumes the antibacterial activity of nano-$Mg(OH)_2$ lies in its ability to penetrate the bacterial cell wall and destroy the structure, leading to cell death. The second mechanism considers moisture adsorption on the $Mg(OH)_2$ nanoparticle surface, which may form a thin meniscus of water as a result of capillarity. The nanoparticles remaining in contact with the bacteria damage the membrane and destroy the cells. It is presently difficult to establish which mechanisms occurred.

4 Conclusions

Homogeneous and well-dispersed magnesium hydroxide filler in a polymer matrix serves as a flame retardant and antibacterial agent. The most favorable effects were recorded for the PP/30% $Mg(OH)_2$ systems. The addition of maleic anhydride as compatibilizer had a positive effect on the mechanical properties (doubling of Young's modulus, without sacrificing tensile strength) and thermal resistance (combustion rate 42% less than pure polypropylene). Maleic anhydride reduced agglomeration during extrusion.

TGA and DTG of PP/10% PP-g-MAH/30% $Mg(OH)_2$ composites showed increased decomposition temperature by approximately 21°C.

The most effective antibacterial activity was found in PP/$Mg(OH)_2$ composites without modifier. Its antibacterial activity is high. Samples with contents of both 10 wt% and 30 wt% produce almost complete absence of bacteria.

Considering their high functional value, research to improve the mechanical and flame retardant properties of PP/$Mg(OH)_2$ composites will continue, as will that in establishing the mechanism of action on bacteria.

Acknowledgements: This work was supported by Poznan University of Technology research grant no. 03/32/443/2014-DS-PB.

References

[1] Dziubek A.M., Kowal A.L., Wat. Sci. Tech., 1983, 15, 155
[2] Kang J., Schwendeman S.P., Biomaterials, 2002, 23, 239
[3] Swarbrick J., Boylan J.J., Encyclopedia of pharmaceutical technology, 3rd edition, Marcel Dekker, New York, 2006
[4] Fellner P., Smarčková E., Pach L., Acta. Chim. Slov., 2009, 2, 14
[5] Giorgi R., Bozzi C., Dei L., Gabbiani C., Ninham B.W., Baglioni P., Langmuir, 2005, 21, 8495
[6] Kumari L., Li W.Z., Vannoy C.H., Leblanc R.M., Wang D.Z., Ceram. Int., 2009, 35, 3355
[7] Meshkani F., Rezaei M., Powder. Technol., 2010, 199, 144
[8] Pilarska A., Markiewicz E., Ciesielczyk F., Jesionowski T., Drying. Technol., 2011, 29, 1210
[9] Dong C., He G., Li H., Zhao R., Han T., Deng Y., J. Membr. Sci., 2012, 388, 40
[10] Al-Hazmi F., Umar A., Dar G.N., Al-Ghamdi A.A., Al-Sayari S.A., Al-Hajry A., et al., J. Alloys. Compd., 2012, 519, 4
[11] Qiu L., Xie R., Ding P., Qu B., Compos. Struct., 2003, 62, 391
[12] Chen X., Yu J., Guo S., Lu S., Luo Z., He M., J. Mater. Sci., 2009, 44, 1324
[13] Gul R., Islam A., Yasin T., Mir S., J. Appl. Polym. Sci., 2011, 121, 2772
[14] Suihkonen R., Nevalainen K., Orell O., Honkanen M., Tang L., Zhang H., et al., J. Mater. Sci., 2012, 47, 1480
[15] Shabanian M., Ghanbari D., J. Appl. Polym. Sci., 2013, 127, 2004
[16] Carrot C., Olalla B., Fulchiron Polymer, 2012, 53, 5560
[17] Rothon R.N., Hornsby P.R., Polym. Degrad. Stab., 1996, 54, 383
[18] Xiang–jian K., Shu–hei L., Jiang–ging Z., J. Cent. South. Univ. Technol., 2008, 15, 779
[19] Morgan A., Wilkie C., Flame Retardant Polymer Nanocomposites, John Wiley & Sons, Inc., Hoboken, New Jersey, 2007
[20] Hui X., Xin-rong D., Trans. Nonferrous Met. Soc. China, 2006, 16, 488
[21] Lv J., Liu W., J. Appl. Polym. Sci., 2007, 105, 333
[22] Ren F., Zhang Z., Wei Z., Chen J., Dong D., Li X., Zhang L., J. Appl. Polym. Sci., 2013, 129, 2261
[23] Jung W.K., Koo H.C., Kim K.W., Sook S., Kim S.H., Park Y.H., Appl. Environ. Microbiol., 2008, 62, 3187
[24] Dong C., Cairney J., Sun Q., Maddan O.L., He G., Deng Y., J. Nanopart. Res., 2010, 12, 2101
[25] Dong C., Song D., Cairney J., Maddan O.L., He G., Deng Y., Mater. Res. Bull., 2011, 46, 576
[26] Al-Hazmi F., Alnowaiser F., Al-Ghamdi A.A., Aly M.M., Al-Tuwirqi R.M., El-Tantawy F., Superlattices Microstruct., 2012, 52, 200
[27] Lei H., Dianqing L., Yanjun L., Evans D.G., Xue D., Chin. Sci. Bull., 2005, 50, 514
[28] Chrzanowski Ł., Ławniczak Ł., Czaczyk K., World J. Microbiol. Biotechnol., 2012, 28, 1
[29] Abdel-Mawgoud A.M., Lepine F., Deziel E., Appl. Microbio. Biotechnol., 2010, 86, 1323
[30] Stone P.W., Expert Rev. Pharmacoecon Outcomes Res., 2009, 9, 417
[31] Li Q., Mahendra S., Lyon D.Y., Brunet L., Liga M.V., Li D., Alvarez P.J., Water. Res., 2008, 42, 4591
[32] Silver S., Phung L.T., Annu. Rev. Microbiol., 1996, 50, 753
[33] Bretani G., J. Bacteriol., 1951, 62, 293
[34] Thi L., Prigent-Combaret C., Methods Enzymol., 2001, 336, 152
[35] Meshkani F., Rezaei M., Powder. Technol., 2009, 196, 85
[36] Pilarska A., Wysokowski M., Markiewicz E., Jesionowski T., Powder. Technol., 2013, 235, 148
[37] Balakrishnan H., Hassan A., Isitman N.A., Kaynak C., Polym. Degrad. Stab., 2012, 97, 1447
[38] Kumari L., Li W.Z., Vannoy C.H., Leblanc R.M., Wang D.Z., Ceram. Inter., 2009, 35, 3355
[39] Bula K., Jesionowski T., Compos. Interface, 2010, 17, 603
[40] Bula K., Jesionowski T., Krysztafkiewicz A., Janik J., Colloid Polym. Sci., 2007, 285, 1267
[41] Chen X., Yu J., Guo S., Luo Z., He M., J. Macromolecular Sci. Part A, 2008, 45, 712
[42] Gibert J.P., Lopez Cuesta J.M., Bergeret A., Crespy A., Polym. Degr. Stab., 2000, 67, 437
[43] Ohira T., Yamamoto O., Chem. Eng. Sci., 2012, 68, 355